

The tZH and tZh production in 2HDM: Prospects for discovery at the LHC

Wei-Shu Hou and Tanmoy Modak

Department of Physics, National Taiwan University, Taipei 10617, Taiwan

We study the discovery potential of the $cg \rightarrow tA \rightarrow tZH$ process at the LHC, where A and H are CP-odd and even exotic scalars, respectively. The context is the general Two Higgs Doublet Model, where $cg \rightarrow tA$ is induced by the flavor changing neutral Higgs coupling ρ_{tc} . We find that the process $cg \rightarrow tA \rightarrow tZH$ can be discovered for $m_A \sim 400$ GeV, but would likely require high luminosity running of the LHC. Such a discovery would shed light on the mechanism behind the observed Baryon Asymmetry of the Universe. We also study $cg \rightarrow tA \rightarrow tZh$, where h is the observed 125 GeV scalar, but find it out of reach at the LHC.

I. INTRODUCTION

The discovery of the Higgs boson [1] $h(125)$ at the Large Hadron Collider (LHC) confirms the Standard Model (SM) as the correct theory at the electroweak scale. As all fermions come in three copies, additional scalars might well exist in Nature. In particular, given that h belongs to a weak doublet Φ , extra scalar doublets ought to be searched for. However, the apparent absence of New Physics (NP) so far at the LHC and the emergent “approximate alignment”, i.e. the h boson is found to resemble rather closely the SM Higgs boson, suggest that the extra scalars might be rather heavy. In this so-called decoupling limit [2], where the exotic scalars are multi-TeV in mass, discovery becomes rather difficult even for the High Luminosity LHC (HL-LHC).

By adding just one scalar doublet Φ' , the two Higgs doublet model (2HDM) [3] is one of the simplest extensions of SM. We are interested in sub-TeV exotic scalars A , H , and H^+ . The most popular 2HDMs, of interest already before the h boson discovery, are those with a Z_2 symmetry imposed [3]. The Z_2 symmetry enforces the up- and down-type quarks to couple to just one scalar doublet, thereby ensuring Natural Flavor Conservation (NFC) [4] and forbids all flavor changing neutral Higgs (FCNH) couplings. But this removes the possibility of any additional Yukawa coupling.

Our context is the general 2HDM (g2HDM), without imposing Z_2 symmetry. Indeed, approximate alignment can be accommodated [5, 6] without taking the decoupling limit, even with $\mathcal{O}(1)$ extra Higgs quartic couplings, clearing the way for sub-TeV A , H , and H^+ . In the absence of Z_2 symmetry, both doublets couple to u - and d -type quarks, and two separate Yukawa matrices $\lambda_{ij}^F = (\sqrt{2}m_i^F/v)\delta_{ij}$ (with $v \simeq 246$ GeV) and ρ_{ij}^F emerge after diagonalization of the fermion mass matrices. Here, F denotes u - and d -type quarks and e -type leptons, with the fermion mass and mixing structure and approximate alignment together replacing the NFC condition [5]. The λ matrices are real and diagonal, but the ρ matrices are in general *non-diagonal* and *complex*. It was pointed out recently that $\mathcal{O}(1)$ ρ_{tt} and ρ_{tc} can drive electroweak baryogenesis (EWBG) rather efficiently [7, 8].

If ρ_{tt} and ρ_{tc} are $\mathcal{O}(1)$, one might discover the exotic scalars via the $cg \rightarrow tA/H \rightarrow tt\bar{c}$ process with clean

same-sign top signature [9, 10] (see also Refs. [11–13]), and also with $A/H \rightarrow t\bar{t}t$, i.e. the triple-top process [9]. Induced by only ρ_{tc} , the same-sign top process might emerge already with full Run-2 data. On the other hand, the more exquisite triple-top process, which depends on both ρ_{tt} and ρ_{tc} couplings, may require the inclusion of Run 3 data to show any indication. But if ρ_{tt} is negligibly small, the triple-top discovery would not be possible. In this paper we consider the case where ρ_{tc} is $\mathcal{O}(1)$ but ρ_{tt} is tiny, where another novel discovery mode would be $cg \rightarrow tA \rightarrow tZH$ (charge conjugate process always implied) for $m_A > m_Z + m_H$. With no dilution from $A \rightarrow t\bar{t}$, the process can provide an additional discovery mode that is complementary to Refs. [9, 10], and provide additional information on ρ_{tc} driven EWBG.

The $cg \rightarrow tA \rightarrow tZH$ process can be searched for in the inclusive $pp \rightarrow tA + X \rightarrow tZH + X$ process, with $Z \rightarrow \ell^+\ell^-$, $H \rightarrow \bar{t}c + t\bar{c}$, and at least one top decaying semileptonically. We call this the tZH process, the observation of which has another intriguing impact. It has been shown that the $A \rightarrow ZH$ decay can provide a smoking gun signature for the strongly first order electroweak phase transition (EWPT) which might have occurred in the early Universe [14–16]. A strongly first order EWPT is needed for the out of equilibrium condition that is required for successful EWBG [17]. Realizing the importance [18], indeed both ATLAS and CMS have pursued $gg \rightarrow A \rightarrow ZH$ search [19, 20]. However, if ρ_{tt} is tiny, $gg \rightarrow A$ vanishes, and the tZH process will be a unique probe of the strongly first order EWPT mechanism, as well as the ρ_{tc} driven EWBG scenario.

For completeness, we also study the prospect for the $cg \rightarrow tA \rightarrow tZh$ process. The process is also induced by ρ_{tc} , but would depend on $\cos\gamma$, the h - H mixing angle. The process can be searched for via $pp \rightarrow tA + X \rightarrow tZh + X$, with $t \rightarrow b\ell^+\nu_\ell$, $Z \rightarrow \ell^+\ell^-$ and $h \rightarrow b\bar{b}$, which we call the tZh process. It provides another complementary probe of the ρ_{tc} driven EWBG scenario, as well as the c_γ mixing angle if ρ_{tt} is rather small.

In the following, we first discuss the framework in Sec. II, followed by the parameter space and discovery potential of the tZH process in Sec. III. Sec. IV is dedicated to the tZh process, and we summarize our results with some discussion in Sec. V.

II. FRAMEWORK

The scalars h , H , A and H^+ couple to fermions by [21]

$$\begin{aligned} \mathcal{L} = & -\frac{1}{\sqrt{2}} \sum_{F=U,D,L'} \bar{F}_i \left[(-\lambda_{ij}^F s_\gamma + \rho_{ij}^F c_\gamma) h \right. \\ & + (\lambda_{ij}^F c_\gamma + \rho_{ij}^F s_\gamma) H - i \operatorname{sgn}(Q_F) \rho_{ij}^F A \left. \right] R F_j \\ & - \bar{U}_i [(V \rho^D)_{ij} R - (\rho^{U\dagger} V)_{ij} L] D_j H^+ \\ & - \bar{\nu}_i \rho_{ij}^L R L'_j H^+ + \text{H.c.}, \end{aligned} \quad (1)$$

where $L, R \equiv (1 \mp \gamma_5)/2$, $i, j = 1, 2, 3$ are generation indices, V is Cabibbo-Kobayashi-Maskawa matrix, $c_\gamma = \cos \gamma$ is the h - H mixing angle between CP-even scalars, and $U = (u, c, t)$, $D = (d, s, b)$, $L' = (e, \mu, \tau)$ and $\nu = (\nu_e, \nu_\mu, \nu_\tau)$ are in vectors in flavor space. The matrices λ_{ij}^F ($= \sqrt{2} m_i^F / v$) are real and diagonal, whereas ρ_{ij}^F are in general complex and non-diagonal.

In the Higgs basis, the most general CP -conserving two Higgs doublet potential can be written as [5, 21]

$$\begin{aligned} V(\Phi, \Phi') = & \mu_{11}^2 |\Phi|^2 + \mu_{22}^2 |\Phi'|^2 - (\mu_{12}^2 \Phi^\dagger \Phi' + \text{h.c.}) \\ & + \frac{\eta_1}{2} |\Phi|^4 + \frac{\eta_2}{2} |\Phi'|^4 + \eta_3 |\Phi|^2 |\Phi'|^2 + \eta_4 |\Phi^\dagger \Phi'|^2 \\ & + \left[\frac{\eta_5}{2} (\Phi^\dagger \Phi')^2 + (\eta_6 |\Phi|^2 + \eta_7 |\Phi'|^2) \Phi^\dagger \Phi' + \text{h.c.} \right], \end{aligned} \quad (2)$$

where the vacuum expectation value v arises from the doublet Φ via the minimization condition $\mu_{11}^2 = -\frac{1}{2} \eta_1 v^2$, while $\langle \Phi' \rangle = 0$ (hence $\mu_{22}^2 > 0$), and η_i s are quartic couplings. Here we follow the notation of Ref. [5]. A second minimization condition, $\mu_{12}^2 = \frac{1}{2} \eta_6 v^2$, removes μ_{12}^2 , and the total number of parameters are reduced to nine [5].

Two relations [5] arise for the mixing angle γ when diagonalizing the mass-squared matrix for h, H ,

$$c_\gamma^2 = \frac{\eta_1 v^2 - m_h^2}{m_H^2 - m_h^2}, \quad \sin 2\gamma = \frac{2\eta_6 v^2}{m_H^2 - m_h^2}. \quad (3)$$

The alignment limit, $c_\gamma \rightarrow 0$, is reached for $\eta_6 \rightarrow 0$ [5], hence $m_h^2 \rightarrow \eta_1 v^2$, or via decoupling [2], i.e. $m_H^2 \gg v^2$. But for small but not infinitesimal c_γ , one has $c_\gamma \simeq |\eta_6| v^2 / (m_H^2 - m_h^2)$. This is the so-called approximate alignment [5], i.e. small c_γ values can be attained with $\eta_6, \eta_1 > m_h^2 / v^2$. The scalar masses can be expressed in terms of the parameters in Eq. (2),

$$\begin{aligned} m_{h,H}^2 = & \frac{1}{2} \left[m_A^2 + (\eta_1 + \eta_5) v^2 \right. \\ & \left. \mp \sqrt{(m_A^2 + (\eta_5 - \eta_1) v^2)^2 + 4\eta_6^2 v^4} \right], \end{aligned} \quad (4)$$

$$m_A^2 = \frac{1}{2} (\eta_3 + \eta_4 - \eta_5) v^2 + \mu_{22}^2, \quad (5)$$

$$m_{H^\pm}^2 = \frac{1}{2} \eta_3 v^2 + \mu_{22}^2. \quad (6)$$

The processes of interest are $cg \rightarrow tA \rightarrow tZH$ and tZh , where $cg \rightarrow tA$ is induced by ρ_{tc} , but the $A \rightarrow ZH, Zh$ decays via the gauge couplings [3, 22]

$$\frac{g_2}{2c_W} Z_\mu [c_\gamma (h \partial^\mu A - A \partial^\mu h) - s_\gamma (H \partial^\mu A - A \partial^\mu H)], \quad (7)$$

with c_W the Weinberg angle and g_2 the $SU(2)_L$ gauge coupling. We see from Eq. (7) that $A \rightarrow ZH$ is proportional to s_γ , while $A \rightarrow Zh$ is proportional to c_γ . The coupling ρ_{ct} can also generate $cg \rightarrow tA$, but it is very stringently constrained by flavor physics [23]. We set ρ_{ct} to zero throughout the paper for simplicity.

For nonzero ρ_{tc} , we remark that the discovery at LHC, if at all, would first occur through the $cg \rightarrow tA \rightarrow tt\bar{c}$ process [9, 10]. For $m_A < 2m_t$, if other ρ_{ijs} are small, $cg \rightarrow tA \rightarrow tZH$ could be the only process to emerge after $cg \rightarrow tA \rightarrow tt\bar{c}$. For $m_A > 2m_t$, $cg \rightarrow tA \rightarrow tt\bar{c}$ would in general be accompanied by the $cg \rightarrow tA \rightarrow t\bar{t}$ process [9], unless ρ_{tt} is negligibly small, which we shall assume. We shall focus on $t \rightarrow b\ell^+\nu_\ell$, $H \rightarrow t\bar{c} + \bar{t}c$, and $Z \rightarrow \ell^+\ell^-$ decays, with the top quark from H decay also decaying semileptonically. Thus, following a possible $cg \rightarrow tA \rightarrow tt\bar{c}$ discovery, $cg \rightarrow tA \rightarrow tZH$ could be the only process that might provide a complementary probe of the ρ_{tc} driven EWBG, even for approximate alignment (i.e. small c_γ) [24]. In the following, we assume ρ_{tc} is the only non-zero coupling and set all other couplings to zero. Their impact, however, will be discussed later in the paper.

The prospect for $cg \rightarrow tA \rightarrow tZh$ closely depends on the mixing angle c_γ , vanishing for $c_\gamma \rightarrow 0$. For large ρ_{tt} , $gg \rightarrow A \rightarrow Zh$ [25] probes c_γ . For negligibly small ρ_{tt} , the process $cg \rightarrow tA \rightarrow tZh$ can provide unique probe of c_γ . We shall focus on $t \rightarrow b\ell^+\nu_\ell$, $h \rightarrow b\bar{b}$ and $Z \rightarrow \ell^+\ell^-$.

III. THE tZH PROCESS

In this section we analyze the discovery potential of the tZH process at the LHC. We first look at the relevant constraints on the parameter space, then find the discovery potential at $\sqrt{s} = 14$ TeV. For simplicity, we assume all $\rho_{ij} = 0$ except ρ_{tc} . However, the impact of other ρ_{ijs} will be discussed later in the paper. To simplify further, we set $c_\gamma = 0$ throughout this section.

A. Parameter Space

Let us find the available parameter space for the tZH process. We first focus on the mass spectrum of the extra scalars A, H and H^+ . The process requires A heavier than H by at least m_Z . To find whether such mass spectrum exists, the dynamical parameters in Eq. (2) need to satisfy positivity, perturbativity, and tree-level unitarity conditions, for which we utilize 2HDMC [26]. We first express the quartic couplings η_1, η_{3-6} in terms of [5, 21]

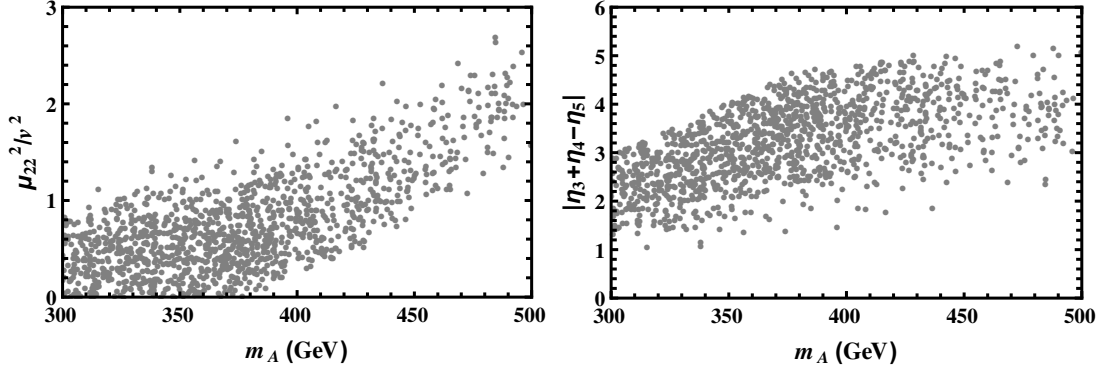


FIG. 1. The scanned points plotted in the μ_{22}^2/v^2 vs m_A (left) and $|\eta_3 + \eta_4 - \eta_5|$ vs m_A (right) plane.

BP	η_1	η_2	η_3	η_4	η_5	η_{345}	η_6	η_7	m_{H^\pm} (GeV)	m_A (GeV)	m_H (GeV)	$\frac{\mu_{22}^2}{v^2}$
<i>a</i>	0.258	2.133	2.87	-0.569	-1.194	1.107	0	-0.791	310	339	207	0.15
<i>b</i>	0.258	1.366	2.718	-0.733	-1.97	0.015	0	-0.252	354	404	208	0.71
<i>c</i>	0.258	2.432	2.67	-0.652	-2.21	-0.192	0	0.091	393	449	260	1.21

TABLE I. Parameter values for the three benchmark points. See text for details.

μ_{22} , m_h , m_H , m_A , m_{H^\pm} , all normalized to v , and the mixing angle γ ,

$$\eta_1 = \frac{m_h^2 s_\gamma^2 + m_H^2 c_\gamma^2}{v^2}, \quad (8)$$

$$\eta_3 = \frac{2(m_{H^\pm}^2 - \mu_{22}^2)}{v^2}, \quad (9)$$

$$\eta_4 = \frac{m_h^2 c_\gamma^2 + m_H^2 s_\gamma^2 - 2m_{H^\pm}^2 + m_A^2}{v^2}, \quad (10)$$

$$\eta_5 = \frac{m_H^2 s_\gamma^2 + m_h^2 c_\gamma^2 - m_A^2}{v^2}, \quad (11)$$

$$\eta_6 = \frac{(m_h^2 - m_H^2)(-s_\gamma)c_\gamma}{v^2}. \quad (12)$$

The quartic couplings η_2 and η_7 do not enter scalar masses, nor the mixing angle γ . Therefore in our analysis we take v , m_h , and γ , m_A , m_H , m_{H^\pm} , μ_{22} , η_2 , η_7 as the phenomenological parameters.

To save computation time, we randomly generate these parameters in the following ranges: $\eta_2 \in [0, 3]$, $\eta_7 \in [-3, 3]$, $\mu_{22} \in [0, 1000]$ GeV, $m_A \in [300, 500]$ GeV, $m_H \in [200, m_A - m_Z]$ GeV, $m_{H^\pm} \in [300, 500]$ GeV, while satisfying $m_h = 125$ GeV. Note that since the $cg \rightarrow tA \rightarrow tZH$ process depends only on s_γ , for simplicity we take $c_\gamma = 0$ in this section. To simplify further, we demand $m_A < m_{H^\pm} + m_W$ to forbid the $A \rightarrow H^\pm W^\mp$ decay. We then pass the randomly generated parameters to 2HDMC for scanning, which uses [26] m_{H^\pm} and Λ_{1-7} as input parameters in the Higgs basis with v as an implicit parameter. To match the 2HDMC convention, we identify η_{1-7} as Λ_{1-7} and take $-\pi/2 \leq \gamma \leq \pi/2$, and η_2 needs to be greater than zero as required by positivity,

along with other more involved conditions in 2HDMC. In addition, we further conservatively demand all $|\eta_i| \leq 3$.

One also has to consider the stringent oblique T parameter [27] constraint, which restricts the scalar masses m_A , m_H , and m_{H^\pm} [28, 29], and therefore the quartic couplings η_i s. We use the T parameter expression given in Ref. [28] and check that the points that passed positivity, unitarity and perturbativity conditions in 2HDMC, also satisfy the T parameter constraint within 2σ error [30]. These final points together are called “scan points”, which are plotted as gray dots in Fig. 1 in the μ_{22}^2/v^2 and $|\eta_3 + \eta_4 - \eta_5|$ vs m_A planes. The figure illustrates that there exists finite parameter space for $300 \text{ GeV} \lesssim m_A \lesssim 500 \text{ GeV}$, which can facilitate $A \rightarrow ZH$ decay. In general, heavier m_A are possible, but the discovery potential diminishes with the rapid fall-off in parton luminosity. From the scan points in Fig. 1, we choose three benchmark points (BPs) for our analysis, which are summarized in Table. I.

The coupling ρ_{tc} is constrained by both LHC search and flavor physics. As we assume $c_\gamma = 0$ throughout this section, the most stringent limit arises from CMS search for four-top production [31], where the CRW region, i.e. Control Region for $t\bar{t}W$ background, gives the most relevant constraint. For non-zero ρ_{tc} , the process $cg \rightarrow tH/tA \rightarrow t\bar{t}\bar{c}$ with same-sign top (same sign leptons plus jets) contributes abundantly to the CRW region, resulting in stringent constraint on ρ_{tc} . There is, however, a subtlety. The $cg \rightarrow tH \rightarrow t\bar{t}\bar{c}$ and $cg \rightarrow tA \rightarrow t\bar{t}\bar{c}$ processes cancel each other exactly by destructive interference, if the masses and widths of H and A are the same [9, 10]. This cancellation diminishes [10] when the $m_A - m_H$ mass splitting is larger than the respec-

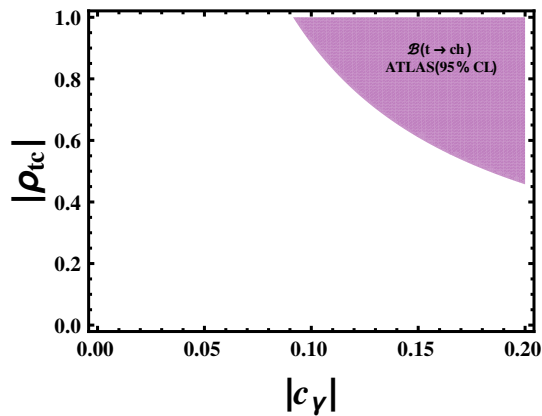


FIG. 2. Constraint from $\mathcal{B}(t \rightarrow ch)$ measurement in ρ_{tc} vs c_γ .

BP	ρ_{tc}	$\mathcal{B}(A \rightarrow t\bar{c} + \bar{c}t)$	$\mathcal{B}(A \rightarrow ZH)$
a	0.4	0.61	0.39
b	0.5	0.41	0.59
c	0.45	0.41	0.59

TABLE II. Branching ratios for the benchmark points.

tive widths, which is the case for all three BPs, where $m_A - m_H$ is more than 100 GeV. We refrain from a detailed discussion on the extraction procedure for this constraint, but refer the reader to Refs. [10, 32]. Following the procedure in Ref. [10] and utilizing the CRW region of Ref. [31], we find the 95% CL upper limit on ρ_{tc} are 0.4, 0.5, 0.45 for the BP a , BP b and BP c respectively.

The constraints from $\mathcal{B}(B \rightarrow X_s \gamma)$ and B_q mixing ($q = d, s$) on ρ_{tc} should also be considered, where ρ_{tc} enters via H^+ coupling in the charm loop [33, 34]. For example, reinterpreting the result of Ref. [33], one finds $|\rho_{tc}| \gtrsim 1$ is excluded for $m_{H^+} = 300$ GeV from B_s mixing, the ballpark mass range for m_{H^+} for all three BPs. The constraints are weaker than those from the CRW region. At this point we remark that, lighter m_A , m_H and, m_{H^\pm} compared to the three BPs are also possible, but the constraints on $|\rho_{tc}|$ from CRW region, $\mathcal{B}(B \rightarrow X_s \gamma)$ and B_q mixing would be more severe.

For nonvanishing c_γ , ρ_{tc} receives further constraints from $\mathcal{B}(t \rightarrow ch)$ measurement. Although we set $c_\gamma = 0$ in this section, let us briefly discuss this constraint. Both ATLAS and CMS have searched for $t \rightarrow ch$ decay and set 95% CL upper limits. The latest ATLAS result is based on 36.1 fb^{-1} data at 13 TeV, setting the limit $\mathcal{B}(t \rightarrow ch) < 1.1 \times 10^{-3}$ [35], while the CMS limit is $\mathcal{B}(t \rightarrow ch) < 4.7 \times 10^{-3}$ [36], based on 35.9 fb^{-1} . The ATLAS constraint on $\mathcal{B}(t \rightarrow ch)$ [35] is illustrated in ρ_{tc} - c_γ plane as the purple shaded region in Fig. 2, where we do not display the weaker CMS limit. Taking $c_\gamma = 0.2$ for example, one gets the upper limit of $|\rho_{tc}| \lesssim 0.5$ at 95% CL [37], but the limit weakens for smaller c_γ .

Under the assumptions made, there are only two decay modes, $A \rightarrow t\bar{c} + \bar{c}t$ and $A \rightarrow ZH$, for all three bench-

mark points. These branching ratios are summarized in Table II, while $\mathcal{B}(H \rightarrow t\bar{c} + \bar{c}t) = 1$. We note that for fixed m_H , $\mathcal{B}(A \rightarrow ZH)$ is larger for heavier m_A , hence $\mathcal{B}(A \rightarrow ZH)$ of BP a is smaller than that of BP b . The total decay widths of A (H) for the three BPs respectively are 2.91 (0.18) GeV, 9.78 (0.29) GeV and, 9.65 (0.98) GeV.

B. Collider Signature

We now analyze the discovery prospects for $cg \rightarrow tA \rightarrow tZH$ at the LHC with $\sqrt{s} = 14$ TeV. The process can be searched for via $pp \rightarrow tA + X \rightarrow tZH + X \rightarrow tZ(t\bar{c} + \bar{c}t) + X$, with $Z \rightarrow \ell^+ \ell^-$ and at least one of the final state top quarks decaying semileptonically. $Z \rightarrow \tau^+ \tau^-$, $\nu \bar{\nu}$ decays are also possible, but we do not find them as promising. The dominant backgrounds for the tZH process arise from $t\bar{t}Z$ and WZ +jets processes, while tWZ , four-top quarks ($4t$), $t\bar{t}h$, $t\bar{t}W$ and tZ +jets are subdominant. Minor contributions come from $3t$ +jets and $3t + W$ jets.

In order to find the discovery potential of the three benchmark points, we generate background and signal event samples at LO by Monte Carlo event generator MadGraph5_aMC@NLO [38] with the parton distribution function (PDF) set NN23LO1 [39] at $\sqrt{s} = 14$ TeV. The event samples are then interfaced with PYTHIA 6.4 [40] for showering and hadronization, and finally fed into Delphes 3.4.0 [41] to incorporate detector effects. We have generated the matrix elements (ME) of signal and all backgrounds except for the WZ +jets with up to one additional jet in the final state, followed by ME and parton shower merging with the MLM matching scheme [42, 43]. We considered two additional jets for ME and parton shower merging for WZ +jets background. We have not included backgrounds arising from the non-prompt and fake sources, as they are not properly modeled in Monte Carlo simulations, and usually require data to make estimates. Here we have incorporated default ATLAS-based detector card available within Delphes framework. The effective model is implemented in FeynRules [44].

The dominant $t\bar{t}Z$ cross section at LO is normalized to the NLO by the K -factor 1.56 [45]. The WZ +jets background is adjusted to NNLO cross section by a factor 2.07 [46]. Furthermore, the LO tZ +jets, $t\bar{t}h$, $4t$ and $t\bar{t}W^-$ ($t\bar{t}W^+$) cross sections are adjusted to NLO by K factors 1.44 [38], 1.27 [47], 2.04 [38] and 1.35 (1.27) [48] respectively, while the cross sections for $3t$ +jets, $3t + W$ jets and tWZ are kept at LO. For simplicity, the QCD correction factors for the tZj and W^+Z +jets processes are assumed to be the same as their respective charge conjugate processes. The signal cross sections for all three BPs are kept at LO.

Let us discuss the event selection criteria for the tZH process. Each event should contain at least three charged leptons (e and μ), at least three jets with at least two b -tagged, and missing transverse energy (E_T^{miss}). The

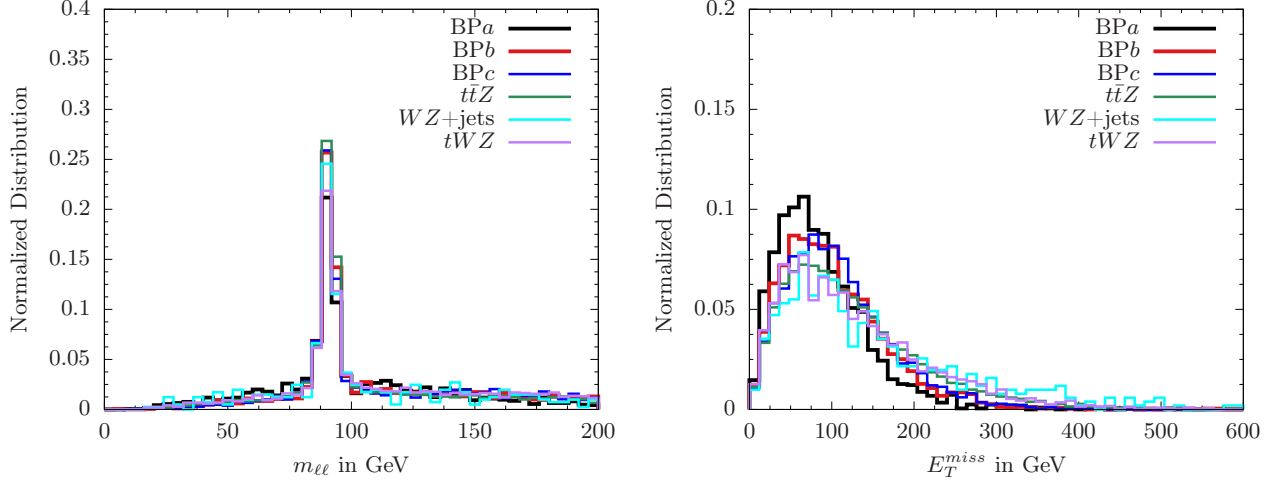


FIG. 3. The normalized $m_{\ell+\ell-}$ (left) and E_T^{miss} (right) distributions for the signal and background processes.

BP	$t\bar{t}Z$	WZ + jets	tWZ	$4t$	$t\bar{t}h$	$t\bar{t}\bar{W}$	tZ + jets	Others	Total Bkg.
a	0.655	0.077	0.025	0.003	0.003	0.003	0.006	0.0001	0.772
b	0.902	0.11	0.035	0.004	0.004	0.004	0.007	0.0002	1.066
c	0.925	0.112	0.036	0.005	0.004	0.004	0.007	0.0002	1.093

TABLE III. Background cross sections (in fb) for the tZH process after selection cuts at $\sqrt{s} = 14$ TeV LHC. The subdominant $3t$ +jets, $3t + W$ are added together as “Others” in the second last column, while the last column is the total background.

transverse momenta, p_T , of the leading charged lepton should be > 25 GeV, while the other two leptons should have $p_T > 20$ GeV. The minimum transverse energy E_T^{miss} needs to be > 35 GeV. All three jets are required to have $p_T > 20$ GeV. The absolute value of pseudo-rapidity, $|\eta|$, of the three leading leptons and three jets (which includes two b -tagged jets) should be < 2.5 . The separation ΔR between any two leptons, any two jets, and any jet and lepton should be > 0.4 . The jets are reconstructed by utilizing anti- k_T algorithm with radius parameter $R = 0.6$.

The invariant mass of the two opposite-charge, same-flavor leptons, $m_{\ell+\ell-}$, is required to be within the Z boson mass window $76 < m_{\ell+\ell-} < 100$ GeV. As there are at least three charged leptons in the event, with two coming from Z decay and one from one of the t quark decays, there will be at least two combinations of $m_{\ell+\ell-}$. We identify the pair having the invariant mass $m_{\ell+\ell-}$ closest to m_Z as the one coming from Z decay, and then impose the $m_{\ell+\ell-}$ mass cut. We finally veto events for $E_T^{\text{miss}} > 150$ GeV, 250 GeV and 270 GeV for BP a , BP b and BP c , respectively. The E_T^{miss} veto helps reduce the dominant $t\bar{t}Z$ background for all three BPs.

The normalized $m_{\ell+\ell-}$ and E_T^{miss} distributions before any selection cuts (with minimal default cuts during event generation in MadGraph5_aMC@NLO) for the three BPs and backgrounds are plotted in Fig. 3.

In this exploratory study, for simplicity we have not optimized the selection cuts such as $m_{\ell+\ell-}$ and E_T^{miss} for our BPs. The background cross sections after selection cuts are summarized in Table III for all three BPs. In Table IV we give signal cross sections and the corresponding significance for the integrated luminosities $\mathcal{L} = 600$ and 3000 fb $^{-1}$. The statistical significances in Table IV are determined by using $\mathcal{Z} = \sqrt{2[(S+B)\ln(1+S/B) - S]}$ [49], where S and B are the number of signal and background events after selection.

BP	Signal (fb)	Significance (\mathcal{Z}) 600 (3000) fb $^{-1}$
a	0.055	1.5 (3.4)
b	0.115	2.7 (6.0)
c	0.092	2.1 (4.8)

TABLE IV. tZH signal cross sections and significances after selection cuts for the three benchmark points.

We find that the significances can reach up to $\sim 1.5\sigma$, 2.7σ and 2.1σ for BP a , BP b and BP c , respectively, for 600 fb $^{-1}$. With the full HL-LHC dataset (i.e. 3000 fb $^{-1}$ integrated luminosity) one can have $\sim 3.4\sigma$, 6σ and 4.8σ for the BPs, respectively. With moderate $S/B \sim 10\%$ for the three BPs, these significances illustrates that dis-

covery is possible for $m_A \sim 400$ GeV, while evidence is possible for $m_A \sim 350$ GeV. The significance is lower for lighter m_A should not be surprising, since $\mathcal{B}(A \rightarrow ZH)$ is lower for BP*a* than BP*b* and BP*c*. For heavier m_A in BP*b* and BP*c*, such enhancement in branching ratios can compensate lower $cg \rightarrow tA$ production cross section due to fall in parton luminosity. Our results illustrate $\sim 2\sigma$ hint is possible for $m_A \sim 400$ GeV at Run 3 (300 fb^{-1}), but discovery would require the HL-LHC. The achievable significances depend mildly on the applied E_T^{miss} veto. E.g., if we apply the same E_T^{miss} veto that is chosen for BP*a* to BP*b* and BP*c*, the significances of the latter two BPs would drop by $\sim 10\%$ and $\sim 17\%$ respectively. However, rejecting events with $E_T^{\text{miss}} > 250$ GeV would enhance the significance for BP*a* by $\sim 18\%$ but reduce by $\sim 8\%$ for BP*c*, while keep the significance for BP*b* unchanged. We remark in our exploratory analysis we have not optimized E_T^{miss} cut and leave out a more detailed analysis for future.

So far we have set all $\rho_{ij} = 0$ except ρ_{tc} . Before closing this subsection, let us briefly discuss the impact of other ρ_{ij} couplings. If ρ_{ij} follows similar flavor organization structure as in SM, ρ_{tt} could be $\mathcal{O}(\lambda_t)$, $\rho_{bb} \sim \lambda_b$, and $\rho_{\tau\tau} \sim \lambda_\tau$. In general, presence of other ρ_{ij} s open up further decay modes of A and H , which in turn dilutes $\mathcal{B}(A \rightarrow ZH)$, and hence the discovery potential of the tZh process. For example, if $\rho_{tt} = \lambda_t$ (0.5), the achievable significances for BP*b* and BP*c* with full HL-LHC dataset are reduced to $\sim 2.7\sigma$ (4.6σ) and 1.7σ (3.3σ), respectively, due to non-zero $\mathcal{B}(A \rightarrow t\bar{t})$. The significance of BP*a* would remain unchanged as $m_A < 2m_t$. Impact of other ρ_{ij} couplings are significantly milder than ρ_{tt} . For example, for $\rho_{bb} \sim \lambda_b$ and $\rho_{\tau\tau} \sim \lambda_\tau$, the significance in Table IV remain practically the same.

Complex ρ_{tt} provides a generally more robust mechanism for EWBG [7, 8]. Having non-zero ρ_{tt} motivates the conventional $gg \rightarrow H \rightarrow t\bar{t}$ scalar resonance search, or $gg \rightarrow Ht\bar{t} \rightarrow t\bar{t}t\bar{t}$ [50] i.e. four-top search. The former process suffers from large interference [51] with the overwhelming $gg \rightarrow t\bar{t}$ background, leading to a peak-dip signature that makes detection difficult, but recent searches by ATLAS [52] and CMS [53] find some sensitivity. See Ref. [32] for a recent discussion in g2HDM context. Presence of both ρ_{tc} and ρ_{tt} can induce $gg \rightarrow A/H \rightarrow t\bar{c}$ [23] and $cg \rightarrow tA/tH \rightarrow t\bar{t}\bar{t}$ processes [9] which can also be observable at the LHC, but the former may suffer from $t+j$ mass resolution, which could be close to 200 GeV [54].

IV. THE tZh PROCESS

We now discuss the prospect of tZh process, i.e. $pp \rightarrow tA+X \rightarrow tZh+X$, with $t \rightarrow b\ell^+\nu_\ell$, $Z \rightarrow \ell^+\ell^-$ ($\ell = e, \mu$), and $h \rightarrow b\bar{b}$. The process depends heavily on the mixing angle c_γ , as well as ρ_{tc} . In addition to the constraint from CMS CRW region [31], it also receives constraint from ATLAS $\mathcal{B}(t \rightarrow ch)$ [35]. Indeed, larger c_γ enhances $\mathcal{B}(A \rightarrow Zh)$, but $cg \rightarrow tA$ production is balanced by the

stronger constraint on ρ_{tc} , as can be seen from Fig. 2. The process is further plagued by tiny $\mathcal{B}(Z \rightarrow \ell^+\ell^-)$. These make the tZh process not as promising as tZH even for HL-LHC, which we make clear in the following.

To find the discovery potential, we choose a benchmark point where A is heavier than $m_h + m_Z$, and lighter than $m_H + m_Z$. Such a choice would forbid $A \rightarrow ZH$ decay and enhance $\mathcal{B}(A \rightarrow Zh)$. Unlike the previous section, we also need $c_\gamma \neq 0$. We find such a benchmark point from 2HDMC which passes the perturbativity, unitarity, positivity constraints, as well as the T parameter constraint. The parameter values are: $\eta_1 = 0.428$, $\eta_2 = 2.88$, $\eta_3 = 0.795$, $\eta_4 = 2.916$, $\eta_5 = 2.334$, $\eta_6 = -0.897$, $\eta_7 = 2.76$, $m_{H^\pm} = 378$ GeV, $m_A = 401$ GeV, $m_H = 559$ GeV, $c_\gamma = 0.186$ and $\mu_{22}^2/v^2 = 1.96$. With this set of parameters, we find ρ_{tc} values above 0.5 is excluded at 95% CL. This is extracted from $\mathcal{B}(t \rightarrow ch)$ [35], while the constraint from CMS CRW region [31] is a bit weaker. The branching ratios corresponding to this BP are $\mathcal{B}(A \rightarrow Zh) \approx 0.1$, $\mathcal{B}(A \rightarrow t\bar{c} + \bar{t}c) \approx 0.9$.

There exists several backgrounds for tZh process. The dominant backgrounds are $t\bar{t}Z$, $4t$, $t\bar{t}h$, with subdominant backgrounds from tZ +jets, $t\bar{t}W$, $3t$ +jets, $3t+W$ jets and tWZ . To find the discovery potential, we follow the same procedure to generate signal and background events as in Sec. III. We keep signal cross section at LO, but for backgrounds we take the same QCD correction factors as in previous section. The details of the selection cuts, and signal and background cross sections after selection cuts, are presented in an Appendix.

The statistical significance at $\sim 1.1\sigma$ turns out to be rather small, even with full HL-LHC dataset. While significances would be lower for heavier m_A due to fall in the parton luminosity, it does not improve much for lighter m_A . In the latter case, i.e. for lighter m_A , $\mathcal{B}(A \rightarrow Zh)$ becomes lower, and the constraint on ρ_{tc} becomes more stringent from CMS CRW region [31]. For $cg \rightarrow tA \rightarrow tZh$ search in $h \rightarrow W^+W^-$ and $Z \rightarrow b\bar{b}$ modes, one loses the mass reconstruction capability of m_Z , m_h and m_A , hence the control of background processes. Therefore, it is likely that the tZh process would remain below sensitivity even for HL-LHC.

V. DISCUSSION AND SUMMARY

We have studied the discovery potential of $cg \rightarrow tA \rightarrow tZH$, tZh processes at the LHC. The tZH process can be discovered, albeit likely needing HL-LHC data. Discovery is possible for $m_A \sim 400$ GeV, with statistical significance reaching up to $\sim 6\sigma$ with full HL-LHC dataset. But m_A cannot be much lighter or heavier than ~ 400 GeV. The discovery prospect for the tZh process is rather limited, primarily due to the suppression from mixing angle c_γ (alignment “protection”), and the constraint on ρ_{tc} from $\mathcal{B}(t \rightarrow ch)$. With significance only about 1σ at best with 3000 fb^{-1} , tZh seems out of reach at the LHC. We note that the $cg \rightarrow tH \rightarrow tZA$ process is pos-

sible for $m_H > m_Z + m_A$, and can be searched for by a strategy similar to tZH . We also remark that ρ_{tu} can induce $ug \rightarrow tA \rightarrow tZH$ process, with similar signature. Although ρ_{tu} could become stringently constrained [55], the discovery potential is balanced by large valence-quark induced $ug \rightarrow tA$ production.

In general, the presence of ρ_{tt} would reduce the discovery potential of tZH because of $\mathcal{B}(A \rightarrow t\bar{t})$, but it opens up other modes for $A \rightarrow ZH$ discovery, for example induce $A \rightarrow ZH$ signal via loop induced $gg \rightarrow A \rightarrow ZH$ [18]. The same is true for ρ_{bb} , where $A \rightarrow ZH$ can be induced by $gb \rightarrow bA \rightarrow bZH$ [56] as well as $gg \rightarrow b\bar{b}A \rightarrow b\bar{b}ZH$ [56, 57]. One can also have $gg \rightarrow A \rightarrow Zh$ [25] and $gg \rightarrow b\bar{b}A \rightarrow b\bar{b}Zh$ [25, 58, 59]. But both processes are again suppressed by the mixing angle c_γ . In general, the impact of ρ_{bb} is inconsequential for the tZH process, but the presence of ρ_{tc} would reduce the discovery potential for ρ_{bb} induced $A \rightarrow ZH$ processes.

We have not discussed so far the uncertainties in our results. We have not included QCD correction factors for signal in both the tZH and tZh processes. In general, c -quark initiated processes have non-negligible systematic uncertainties such as from PDF, which we have not included in our analysis. Such uncertainties for c -quark initiated processes are discussed in Refs. [60, 61], while a detailed discussion of PDF choices and their uncertainties for Run 2 can be found in Ref. [62]. These lead to some uncertainties in our results. A detailed estimate of such uncertainties is beyond the scope of this paper.

While the presence of ρ_{tt} reduces the discovery potential of the tZH process $m_A > 2m_t$, it opens up the exquisite discovery mode $cg \rightarrow tA/tH \rightarrow t\bar{t}\bar{t}$. It is also worthy of mention the “excess” seen by CMS [53] in $gg \rightarrow A \rightarrow t\bar{t}$ search at $m_A \approx 400$ GeV. Such excess can be interpreted within g2HDM framework [32], if $\rho_{tt} \simeq 1.1$ and $\rho_{tc} \simeq 0.9$ with $m_{H^\pm} \gtrsim 530$ GeV and $m_H \gtrsim 500$ GeV. Note that, for $\rho_{tt} \sim 1$, the tZH discovery (or $cg \rightarrow tH \rightarrow tZA$ discovery) is not possible due to suppression from $\mathcal{B}(A \rightarrow t\bar{t})$ ($\mathcal{B}(H \rightarrow t\bar{t})$) decay. However, if this excess materializes into evidence or discovery by Run 3, $cg \rightarrow tA/tH \rightarrow t\bar{t}\bar{t}$ might emerge immediately followed by discovery of $cg \rightarrow tA/tH \rightarrow t\bar{t}\bar{t}$.

In Summary, motivated by electroweak baryogenesis, we analyzed the discovery potential of the $cg \rightarrow tA \rightarrow tZH$ process. Such process might be induced by extra Yukawa coupling ρ_{tc} if one removes the discrete Z_2 symmetry from 2HDM. We find discovery is possible at the HL-LHC if $m_A \sim 400$ GeV, but ρ_{tt} would need to

be small. For completeness, we have also studied the $cg \rightarrow tA \rightarrow tZh$ process, but do not find it promising. Discovery of the $cg \rightarrow tA \rightarrow tZH$ process will not only shed light on the strongly first order electroweak phase transition, it may also help uncover the mechanism behind the observed Baryon Asymmetry of the Universe.

ACKNOWLEDGMENTS

This research is supported by grants from MOST 106-2112-M-002-015-MY3, 107-2811-M-002-039, NTU 108L104019, and MOST 108-2811-M-002-537.

Appendix A: Event selection for the tZh process

We discuss the event selection criteria and the corresponding signal and backgrounds for the tZh process. Events are required to have at least three leptons, and at least three b -jets with some missing transverse energy. The p_T of the leading and other two subleading leptons are required to be $> 25, 20$ and 15 GeV respectively, with pseudo-rapidity $|\eta| < 2.5$. The p_T of all three b -jets are required to be > 20 GeV with $|\eta| < 2.5$. The E_T^{miss} in each event should be > 35 GeV. We demand the separation ΔR between any two leptons, any two jets, and any jet and lepton to be > 0.4 . We then apply the $m_{\ell+\ell^-}$ cut: for each event there are at least two possible $m_{\ell+\ell^-}$ combinations, and the $m_{\ell+\ell^-}$ combination closest to m_Z should be within $70 \text{ GeV} < m_{\ell+\ell^-} < 100 \text{ GeV}$. Similarly, there are at least two possible m_{bb} combinations in each event. We demanded the one that is closest to m_h should be within $|m_{bb} - m_h| < 25 \text{ GeV}$. Finally, we construct all possible $m_{\ell\ell bb}$ combinations from the three leading leptons and leading b -jets, and demand the $m_{\ell\ell bb}$ combination closest to m_A should be within $|m_{\ell\ell bb} - m_A| < 100 \text{ GeV}$. The cross sections of signal and background processes after selection cuts are summarized in Table V.

Signal (fb)	$t\bar{t}Z$	$4t$	$t\bar{t}\bar{h}$	Others	Total Bkg.
0.003	0.025	0.002	0.0001	0.0001	0.027

TABLE V. Signal and background cross sections (in fb) for the tZh process after selection cuts at $\sqrt{s} = 14$ TeV LHC. The subdominant backgrounds are added together as “Others”, and the last column is the total background.

- [1] G. Aad *et al.* [ATLAS Collaboration], Phys. Lett. B **716**, 1 (2012); S. Chatrchyan *et al.* [CMS Collaboration], *ibid.* B **716**, 30 (2012).
[2] J.F. Gunion and H.E. Haber, Phys. Rev. D **67**, 075019 (2003).

- [3] See e.g. G.C. Branco, P.M. Ferreira, L. Lavoura, M.N. Rebelo, M. Sher and J.P. Silva, Phys. Rept. **516**, 1 (2012); and references there in.
[4] S.L. Glashow and S. Weinberg, Phys. Rev. D **15**, 1958 (1977).

- [5] W.-S. Hou and M. Kikuchi, *Eur. Phys. Lett.* **123**, 11001 (2018).
- [6] See also, e.g. J. Bernon, J.F. Gunion, H.E. Haber, Y. Jiang and S. Kraml, *Phys. Rev. D* **92**, 075004 (2015); P. Bechtle *et al.*, *Eur. Phys. J. C* **77**, 67 (2017).
- [7] K. Fuyuto, W.-S. Hou, E. Senaha, *Phys. Lett. B* **776**, 402 (2018).
- [8] See also J. de Vries, M. Postma, J. van de Vis and G. White, *JHEP* **1801**, 089 (2018).
- [9] M. Kohda, T. Modak, W.-S. Hou, *Phys. Lett. B* **776**, 379 (2018).
- [10] W.-S. Hou, M. Kohda, T. Modak, *Phys. Lett. B* **786**, 212 (2018).
- [11] W.-S. Hou, G.-L. Lin, C.-Y. Ma, C.-P. Yuan, *Phys. Lett. B* **409**, 344 (1997).
- [12] S. Iguro, K. Tobe, *Nucl. Phys. B* **925**, 560 (2017).
- [13] Without detailed studies, the process was also discussed by W. Altmannshofer *et al.*, *Phys. Rev. D* **94**, 115032 (2016); W. Altmannshofer, B. Maddock and D. Tucker, *ibid.* **D 100**, 015003 (2019); and Ref. [12]. See also S. Gori, C. Grojean, A. Juste and A. Paul, *JHEP* **1801**, 108 (2018), where the $pp \rightarrow t\bar{c}H$ process was discussed.
- [14] N. Turok and J. Zadrozny, *Nucl. Phys. B* **358**, 471 (1991).
- [15] L. Fromme, S.J. Huber and M. Seniuch, *JHEP* **0611**, 038 (2006).
- [16] G.C. Dorsch, S.J. Huber, K. Mimasu and J.M. No, *Phys. Rev. Lett.* **113**, 211802 (2014).
- [17] A.G. Cohen, D.B. Kaplan and A.E. Nelson, *Ann. Rev. Nucl. Part. Sci.* **43**, 27 (1993).
- [18] For a non-exhaustive list, see e.g. B. Coleppa, F. Kling and S. Su, *JHEP* **1409**, 161 (2014); B. Hespel, F. Maltoni and E. Vryonidou, *JHEP* **1506**, 065 (2015); F. Kling, H. Li, A. Pyarelal, H. Song and S. Su, *JHEP* **1906**, 031 (2019).
- [19] M. Aaboud *et al.* [ATLAS Collaboration], *Phys. Lett. B* **783**, 392 (2018).
- [20] V. Khachatryan *et al.* [CMS Collaboration], *Phys. Lett. B* **759**, 369 (2016).
- [21] See, e.g., S. Davidson and H.E. Haber, *Phys. Rev. D* **72**, 035004 (2005).
- [22] A. Djouadi, *Phys. Rept.* **459**, 1 (2008).
- [23] B. Altunkaynak *et al.*, *Phys. Lett. B* **751**, 135 (2015).
- [24] D. Chowdhury and O. Eberhardt, *JHEP* **1805**, 161 (2018); J. Haller, A. Hoecker, R. Kogler, K. Mönig, T. Peiffer and J. Stelzer (Gitter Group), *Eur. Phys. J. C* **78**, 675 (2018). See also W.-S. Hou, M. Kohda and T. Modak, *Phys. Rev. D* **98**, 075007 (2018).
- [25] M. Aaboud *et al.* [ATLAS Collaboration], *JHEP* **1803**, 174 (2018); A.M. Sirunyan *et al.* [CMS Collaboration], *Eur. Phys. J. C* **79**, 564 (2019); and references therein.
- [26] D. Eriksson, J. Rathsman and O. Stål, *Comput. Phys. Commun.* **181**, 189 (2010).
- [27] M.E. Peskin and T. Takeuchi, *Phys. Rev. D* **46**, 381 (1992).
- [28] H.E. Haber and O. Stål, *Eur. Phys. J. C* **75**, 491 (2015).
- [29] C.D. Froggatt, R.G. Moorhouse and I.G. Knowles, *Phys. Rev. D* **45**, 2471 (1992).
- [30] M. Baak and R. Kogler, arXiv:1306.0571 [hep-ph].
- [31] A.M. Sirunyan *et al.* [CMS Collaboration], arXiv:1908.06463 [hep-ex].
- [32] W.-S. Hou, M. Kohda and T. Modak, *Phys. Lett. B* **798**, 134953 (2019).
- [33] A. Crivellin, A. Kokulu, C. Greub, *Phys. Rev. D* **87**, 094031 (2013).
- [34] S.-P. Li, X.-Q. Li and Y.-D. Yang, *Phys. Rev. D* **99**, 035010 (2019).
- [35] M. Aaboud *et al.* [ATLAS Collaboration], *JHEP* **1905**, 123 (2019).
- [36] A. M. Sirunyan *et al.* [CMS Collaboration], *JHEP* **1806**, 102 (2018).
- [37] W.-S. Hou, M. Kohda and T. Modak, *Phys. Rev. D* **99**, 055046 (2019).
- [38] J. Alwall *et al.*, *JHEP* **1407**, 079 (2014).
- [39] R.D. Ball *et al.* [NNPDF Collaboration], *Nucl. Phys. B* **877**, 290 (2013).
- [40] T. Sjöstrand, S. Mrenna and P. Skands, *JHEP* **0605**, 026 (2006).
- [41] J. de Favereau *et al.* [DELPHES 3 Collaboration], *JHEP* **1402**, 057 (2014).
- [42] M.L. Mangano, M. Moretti, F. Piccinini and M. Treccani, *JHEP* **0701**, 013 (2007).
- [43] J. Alwall *et al.*, *Eur. Phys. J. C* **53**, 473 (2008).
- [44] A. Alloul, N.D. Christensen, C. Degrande, C. Duhr and B. Fuks, *Comput. Phys. Commun.* **185**, 2250 (2014).
- [45] J. Campbell, R.K. Ellis and R. Röntsch, *Phys. Rev. D* **87**, 114006 (2013).
- [46] M. Grazzini, S. Kallweit, D. Rathlev and M. Wiesemann, *Phys. Lett. B* **761**, 179 (2016).
- [47] SM Higgs production cross sections at $\sqrt{s} = 14$ TeV: <https://twiki.cern.ch/twiki/bin/view/LHCPhysics/CERNYellowReportPageAt14TeV2010>.
- [48] J.M. Campbell and R.K. Ellis, *JHEP* **1207**, 052 (2012).
- [49] G. Cowan, K. Cranmer, E. Gross and O. Vitells, *Eur. Phys. J. C* **71**, 1554 (2011).
- [50] See e.g. N. Craig *et al.*, *JHEP* **1506**, 137 (2015); S. Kanemura, H. Yokoya, Y.-J. Zheng, *Nucl. Phys. B* **898**, 286 (2015); S. Gori *et al.*, *Phys. Rev. D* **93**, 075038 (2016); N. Craig *et al.*, *JHEP* **1701**, 018 (2017). These studies are for 2HDM with softly-broken Z_2 symmetry.
- [51] For a recent reference, see M. Carena and Z. Liu, *JHEP* **1611**, 159 (2016); and references therein.
- [52] M. Aaboud *et al.* [ATLAS Collaboration], *Phys. Rev. Lett.* **119**, 191803 (2017).
- [53] A.M. Sirunyan *et al.* [CMS Collaboration], arXiv:1908.01115 [hep-ex].
- [54] K.-F. Chen, private communication. See e.g. the m_{tj} resolution in excited top search, A.M. Sirunyan *et al.* [CMS Collaboration], *Phys. Lett. B* **778**, 349 (2018).
- [55] W.-S. Hou, M. Kohda, T. Modak and G.-G. Wong, arXiv:1903.03016 [hep-ph].
- [56] T. Modak, *Phys. Rev. D* **100**, 035018 (2019).
- [57] T. Modak and E. Senaha, *Phys. Rev. D* **99**, 115022 (2019).
- [58] P.M. Ferreira, S. Liebler and J. Wittbrodt, *Phys. Rev. D* **97**, 055008 (2018).
- [59] N.M. Coyle, B. Li and C.E.M. Wagner, *Phys. Rev. D* **97**, 115028 (2018).
- [60] M. Buza, Y. Matiounine, J. Smith and W.L. van Neerven, *Eur. Phys. J. C* **1**, 301 (1998).
- [61] F. Maltoni, G. Ridolfi and M. Ubiali, *JHEP* **1207**, 022 (2012).
- [62] J. Butterworth *et al.*, *J. Phys. G* **43**, 023001 (2016). See also W.-S. Hou, M. Kohda and T. Modak, *Phys. Rev. D* **98**, 015002 (2018).